Acta Crystallographica Section F
Structural Biology Communications
ISSN 2053-230X

Purification, crystallization and preliminary X-ray analysis of the inverse F-BAR domain of the human srGAP2 protein

Hongpeng Wang,[a,b] Yan Zhang,[a,b] Zhenyi Zhang,[a,b] Wei-Lin Jin[b]* and Geng Wu[a,b]*

[a]State Key Laboratory of Microbial Metabolism, Shanghai Jiao Tong University, Shanghai 200240, People's Republic of China, and [b]School of Life Sciences and Biotechnology, Shanghai Jiao Tong University, Shanghai 200240, People's Republic of China

Correspondence e-mail: weilinjin@sjtu.edu.cn, geng.wu@sjtu.edu.cn

Received 26 September 2013
Accepted 12 December 2013

Bin–Amphiphysin–Rvs (BAR) domain proteins play essential roles in diverse cellular processes by inducing membrane invaginations or membrane protrusions. Among the BAR superfamily, the 'classical' BAR and Fes/CIP4 homology BAR (F-BAR) subfamilies of proteins usually promote membrane invaginations, whereas the inverse BAR (I-BAR) subfamily generally incur membrane protrusions. Despite possessing an N-terminal F-BAR domain, the srGAP2 protein regulates neurite outgrowth and neuronal migration by causing membrane protrusions reminiscent of the activity of I-BAR domain proteins. In this study, the inverse F-BAR (IF-BAR) domain of human srGAP2 was overexpressed, purified and crystallized. The crystals of the srGAP2 IF-BAR domain protein diffracted to 3.50 Å resolution and belonged to space group $P2_1$. These results will facilitate further structural determination of the srGAP2 IF-BAR domain and the ultimate elucidation of its peculiar behaviour of inducing membrane protrusions rather than membrane invaginations.

1. Introduction

The BAR (Bin, Amphiphysin and Rvs) domain superfamily of proteins plays important roles in a vast array of cellular processes including organelle biogenesis, cell division, cell migration, secretion and endocytosis (Frost *et al.*, 2009; Rao & Haucke, 2011). The crystal structures of several BAR domains from different proteins have been determined (Tarricone *et al.*, 2001; Lee *et al.*, 2007). Based on their functions and sequence homologies, the BAR domain superfamily can be divided into three different subfamilies: the 'classical' BARs/N-BARs such as arfaptin (PDB entry 1i49; Tarricone *et al.*, 2001), the F-BARs (Fes/CIP4 homology-BAR) such as Cdc42-interacting protein 4 (PDB entry 2efk; Shimada *et al.*, 2007) and the I-BARs (inverse BARs) such as missing-in-metastasis (MIM; PDB entry 2d1l; Lee *et al.*, 2007). The BAR and F-BAR subfamilies of proteins generate membrane invaginations during processes such as clathrin-mediated endocytosis (Frost *et al.*, 2008; Itoh *et al.*, 2005), whereas the I-BAR subfamily of proteins such as MIM and IRSp53 produces membrane protrusions which form filopodia *in vitro* and in living cells (Mattila *et al.*, 2007).

Slit-Robo GTPase-activating protein 2 (srGAP2) regulates neurite outgrowth, axon branching, neuronal migration and morphogenesis through its N-terminal F-BAR domain (Carlson & Soderling, 2009; Guerrier *et al.*, 2009; Coutinho-Budd *et al.*, 2012; Ma *et al.*, 2013). Although it possesses an N-terminal F-BAR domain, surprisingly it was found that it employs its F-BAR domain to induce filopodia-like membrane protrusions similar to those induced by I-BAR proteins (Guerrier *et al.*, 2009). Therefore, we name it an inverse F-BAR (IF-BAR) domain protein, so as to emphasize its difference from regular F-BAR proteins. There is no structural information available for this peculiar IF-BAR domain protein and it is unknown how srGAP2 employs its IF-BAR domain to promote membrane protrusions instead of membrane invaginations. In the PDB, its closest homologue among the F-BAR domain superfamily is the EFC_{FBP17} F-BAR domain (PDB entry 2efl; Shimada *et al.*, 2007), which displays only 19% sequence homology to srGAP2 IF-BAR.

In this study, we overexpressed, purified and crystallized the IF-BAR domain of human srGAP2. In addition, we collected diffraction

data from crystals of the human srGAP2 IF-BAR domain, which were processed to 3.50 Å resolution. These studies provide a basis for the ultimate structural determination of the IF-BAR domain of srGAP2, which will shed light on the interesting mechanism of how this unique IF-BAR domain protein induces membrane protrusions, filopodia formation and neurite outgrowth.

2. Materials and methods

2.1. Cloning and protein expression

cDNA sequences encoding the IF-BAR domain of human srGAP2 (residues 1–488 and residues 15–347) were amplified by PCR and cloned into the *Bam*HI and *Not*I restriction-enzyme sites of multiple cloning site 1 (MCS-1) of the expression vector pRSFDuet-1 (Novagen) using standard molecular-cloning procedures. Three additional residues, Gln-Asp-Pro, were introduced between the His tag and protein through the cloning procedure. Successfully cloned plasmids were verified by sequencing. The human srGAP2 IF-BAR domain constructs were expressed as N-terminally His-tagged proteins in *Escherichia coli* strain BL21(DE3). When the OD_{600} reached 0.6–0.8, the bacterial cultures were induced with 0.2 m*M* isopropyl β-D-1-thiogalactopyranoside (IPTG) and grown for a further 16–18 h at 298 K. The bacterial cells were then harvested by centrifugation at 2500*g* for 20 min.

2.2. Protein purification

The cell pellets were homogenized in buffer *A* (25 m*M* Tris–HCl pH 8.0, 300 m*M* NaCl, 20 m*M* imidazole), which was supplemented with 1 µg ml^{-1} aprotinin, 1 µg ml^{-1} leupeptin, 30 µg ml^{-1} lysozyme and 0.05 m*M* phenylmethylsulfonyl fluoride (PMSF). After lysis by sonication, the cell debris was removed by centrifugation at 15 000*g* for 30 min at 277 K. The supernatant was passed through a nickel-affinity column (GE Healthcare) pre-equilibrated with 50 column volumes of buffer *A*. The column was then washed with a further 50 column volumes of buffer *A* and eluted with five column volumes of buffer *B* (25 m*M* Tris–HCl pH 8.0, 300 m*M* NaCl, 60 m*M* imidazole) and 30 column volumes of buffer *C* (25 m*M* Tris–HCl pH 8.0, 300 m*M* NaCl, 140 m*M* imidazole). The target protein was further purified by gel-filtration chromatography using a Superdex 200 10/300 GL column (GE Healthcare) pre-equilibrated with 10 m*M* MES pH 6.0, 150 m*M* NaCl, 2 m*M* dithiothreitol (DTT). The purity of the finally purified protein was verified by SDS–PAGE with Coomassie Blue staining. Peak fractions from the Superdex 200 gel-filtration chromatography were combined and concentrated to 10 mg ml^{-1}, frozen in liquid nitrogen and stored at 193 K for crystallization.

2.3. Crystallization

Crystallization trials for the IF-BAR domain of human srGAP2 were performed at 287 K using the hanging-drop vapour-diffusion method in 48-well plates. Typically, 1 µl protein solution was mixed with 1 µl reservoir solution and equilibrated against 200 µl reservoir solution. Initial crystallization screening trials were performed using Crystal Screen and Crystal Screen 2 (98 conditions), Index (96 conditions), PEGRx 1 and 2 (96 conditions), SaltRx 1 and 2 (96 conditions) and PEG/Ion and PEG/Ion 2 (96 conditions) kits from Hampton Research, and were followed by crystallization screening trials using JBScreen Classic 1–10 (24 × 10 = 240 conditions), JBScreen Basic 1–4 (24 × 4 = 96 conditions) and JBScreen PEG/Salt 1–4 (24 × 4 = 96 conditions) from Jena Bioscience, Wizard Screen I, II, III and IV (96 × 4 = 392 conditions) from Emerald BioSystems and 32 home-made crystallization screen kits (32 × 12 = 384 conditions) at five different temperatures (277, 281, 287, 292 and 297 K). After three weeks, small crystals of the IF-BAR domain of srGAP2 (15–347) were obtained from condition No. 15 of PEG/Ion 2, which consists of 12% PEG 3350, 4% Tacsimate pH 7.0. After further optimization, diffracting crystals were obtained with 12% PEG 3350, 4% Tacsimate pH 7.0, 4% 1,2-butanediol, still using the hanging-drop vapour-diffusion method in 48-well plates at 287 K.

2.4. Data collection

Prior to data collection, human srGAP2 (15–347) protein crystals were cryoprotected by direct transfer in cryoloops into a cryoprotectant which consisted of reservoir solution supplemented with 25%(*v*/*v*) glycerol by replacing the water in the crystallant with the cryoprotectant. The crystals were then flash-cooled in liquid nitrogen and tested on an in-house X-ray generator at Shanghai Institute of Organic Chemistry, where they diffracted to a resolution of approximately 4.3 Å. A complete diffraction data set was collected on BL17U1 at the Shanghai Synchrotron Radiation Facility, Shanghai, People's Republic of China. The data set was collected at a wavelength of 0.98397 Å using an ADSC Quantum 315r CCD area detector and was processed to 3.50 Å resolution. Intensity data were integrated and scaled using the *HKL*-2000 software (Otwinowski & Minor, 1997).

3. Results and discussion

The recombinant IF-BAR domain (residues 1–488) of human srGAP2 (GenBank accession No. AAI44344), with an estimated molecular weight of 57 kDa, was overexpressed as an N-terminally His-tagged protein and purified by Ni^{2+}-affinity chromatography and gel-filtration chromatography. Our gel-filtration chromatography results showed that the srGAP2 (1–488) protein eluted as an approximately 120 kDa protein (Fig. 1*a*), suggesting that srGAP2 (1–488) exists as a dimer in solution.

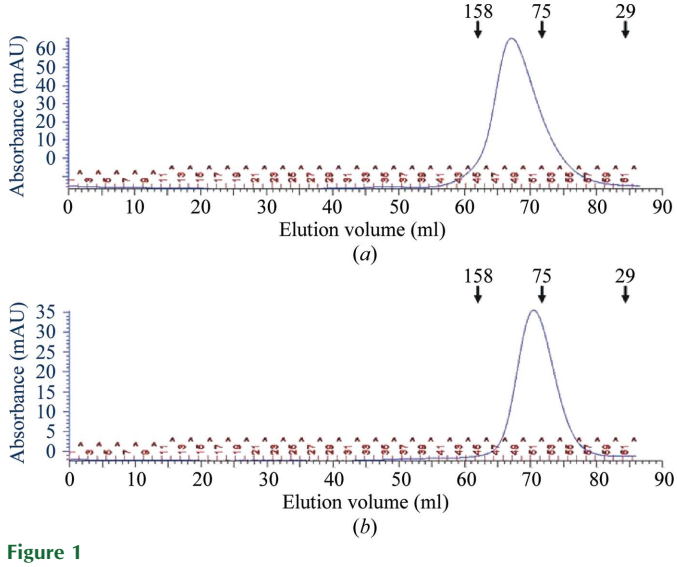

Figure 1
Gel-filtration chromatography profiles for the human srGAP2 IF-BAR domain protein. (*a*) Gel-filtration chromatography profile for human srGAP2 (residues 1–488) protein. Elution volumes of the standard molecular-weight marker are indicated above the chromatogram. (*b*) Gel-filtration chromatography profile for human srGAP2 (residues 15–347) protein.

The purified IF-BAR domain of srGAP2 (1–488) was subjected to extensive crystallization screening. Despite considerable effort and extensive crystallization trials, crystals of the srGAP2 (1–488) protein could not be obtained. Our sequence-alignment result indicated that the first 14 residues are not conserved compared with its homologues. Therefore, a construct of human srGAP2 (15–347) with an estimated molecular weight of 40 kDa was generated. The srGAP2 (15–347) protein was overexpressed and purified using the same procedure as that used for srGAP2 (1–488) (Figs. 1*b* and 2). Gel-filtration chromatography results indicated that srGAP2 (15–347) also exists as a dimer in solution (Fig. 1*b*). Crystallization screening and further optimization of the crystallization conditions yielded rod-shaped crystals (Fig. 3). It is possible that the noncleavable His tag might have impeded crystallization of our protein. We tried introducing the 3C protease cleavage site into the MCS, cleaving off the His tag with 3C protease and performing a crystallization screen for purified srGAP2 IF-BAR domain protein without a His tag. Unfortunately, we have not yet been able to obtain good diffracting crystals using this method.

Crystals of the human srGAP2 IF-BAR domain protein (residues 15–347) diffracted to 3.50 Å resolution (Fig. 4) and belonged to the monoclinic space group $P2_1$, with unit-cell parameters a = 92.1, b = 56.4, c = 95.4 Å, β = 101.8°. Diffraction data were collected and processed with a final $R_{\rm meas}$ value of 12.1% (93.5% for the highest resolution shell) (Table 1).

Based on calculation of the Matthews coefficient (Matthews, 1968), the most probable number of molecules of srGAP2 (15–347) in each asymmetric unit is two, which is consistent with our gel-filtration

Table 1
Data-collection statistics.

Values in parentheses are for the outermost resolution shell.

Beamline	BL17U1
Beam size (µm)	70 × 50
Wavelength (Å)	0.98357
Crystal-to-detector distance (mm)	400
Data-collection temperature (K)	100
Oscillation range per frame (°)	1
Exposure time per frame (s)	1
Images taken	180
Resolution (Å)	50–3.50 (3.63–3.50)
Space group	$P2_1$
Mosaicity (°)	1.1–2.2
Unit-cell parameters (Å, °)	a = 92.1, b = 56.4, c = 95.4, α = 90, β = 101.8, γ = 90
Estimated No. of molecules per asymmetric unit	2
Matthews coefficient (Å^3 Da^{-1})	3.24
Solvent content (%)	62.1
No. of observed reflections	44831
No. of unique reflections	12321
Completeness (%)	99.5 (99.8)
Multiplicity	3.6 (3.7)
Average $I/\sigma(I)$	11.2 (1.5)
$R_{\rm merge}$† (%)	10.3 (79.7)
$R_{\rm meas}$ (%)	12.1 (93.5)
$CC_{1/2}$ for the highest resolution shell (%)	67.3

† $R_{\rm merge} = \sum_{hkl}\sum_i |I_i(hkl) - \langle I(hkl)\rangle| / \sum_{hkl}\sum_i I_i(hkl)$, where $I_i(hkl)$ is the intensity of observation i of reflection hkl.

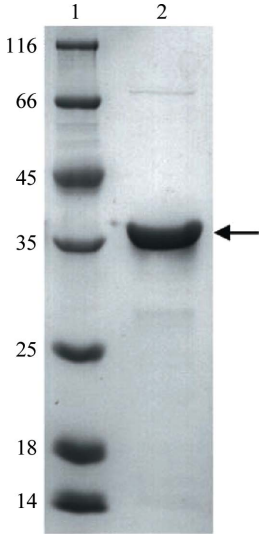

Figure 2
The final purified IF-BAR domain of human srGAP2 protein (residues 15–347). Protein samples were analyzed using 12% SDS–PAGE followed by Coomassie Blue staining. Lane 1, protein molecular-mass marker (labelled in kDa). Lane 2, the final purified protein after the gel-filtration chromatography step. The arrow indicates the band corresponding to the F-BAR domain of human srGAP2 protein (residues 15–347).

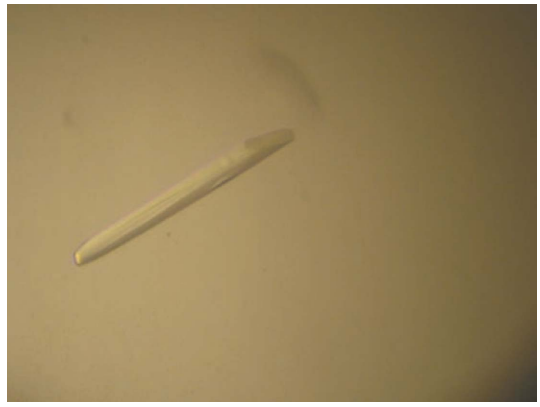

Figure 3
A single crystal of the IF-BAR domain of human srGAP2 protein (residues 15–347). The maximum dimensions of the crystals are 0.05 × 0.05 × 0.45 mm.

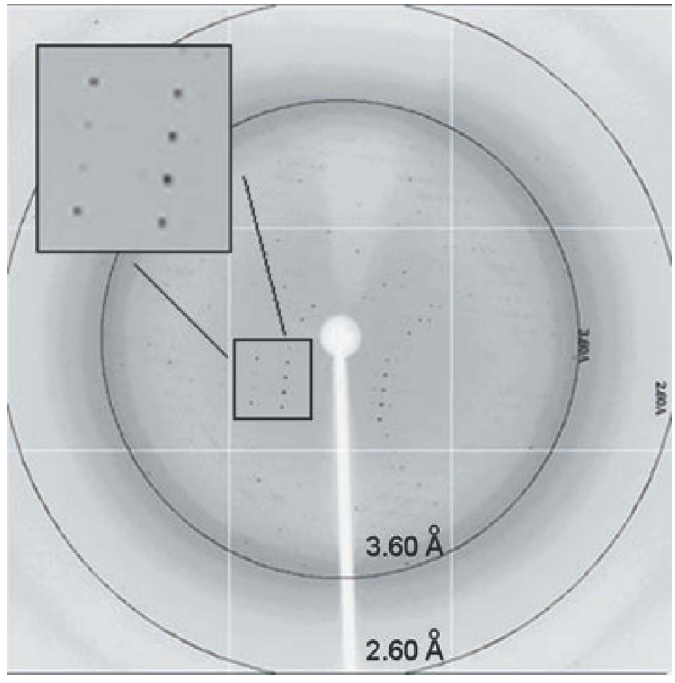

Figure 4
A typical X-ray diffraction image of the IF-BAR domain of human srGAP2 protein (residues 15–347). The crystal diffraction data set was processed to 3.50 Å resolution using the *HKL*-2000 software (Otwinowski & Minor, 1997).

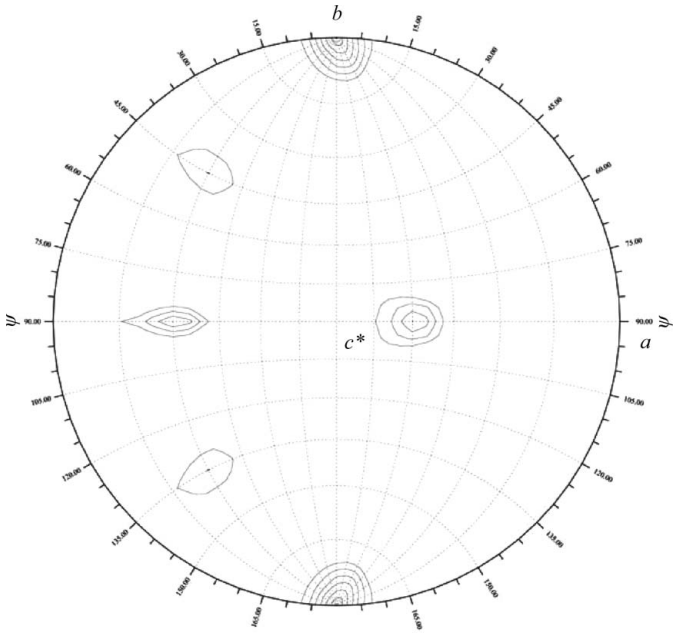

Figure 5
A stereographic projection of the $\kappa = 180^\circ$ section of the calculated self-rotation function of the processed diffraction data.

chromatography results, suggesting that it exists as a dimer in solution. In this case, the Matthews coefficient is 3.24 Å^3 Da^{-1}, corresponding to a solvent content of 62.1% (Table 1). Calculation of the self-rotation function indicated a twofold noncrystallographic symmetry (NCS) axis (Fig. 5). We attempted to determine the crystal structure of the IF-BAR domain of srGAP2 by the molecular-replacement method with the *CCP*4 program *Phaser* (McCoy *et al.*, 2007) using the reported structure of the EFC_{FBP17} F-BAR domain (PDB entry 2efl; Shimada *et al.*, 2007) as a search model, but our efforts were unsuccessful. The EFC_{FBP17} F-BAR domain, which is closest to the IF-BAR domain of srGAP2 in the PDB, exhibits a mere 19% sequence identity to the IF-BAR of human srGAP2. Therefore, experimental phasing approaches such as using selenomethionine-substituted protein crystals to collect multi-wavelength or single-wavelength anomalous dispersion data sets might be required to solve this structure. Elucidation of the crystal structure of the IF-BAR domain of human srGAP2 will provide new insights into the interesting mechanism of how this unique F-BAR domain protein induces membrane protrusions, filopodia formation and neurite outgrowth.

We thank Dr Jiahai Zhou (Shanghai Institute of Organic Chemistry) for assistance in the screening for high-quality diffracting crystals. We also thank the staff of beamline BL17U1 at the Shanghai Synchrotron Radiation Facility for assistance during the data-collection process. This work was supported by grants from the National Natural Science Foundation of China (31230002 to GW and 31171033 to W-LJ).

References

Carlson, B. & Soderling, S. H. (2009). *Dev. Cell*, **17**, 307–309.
Coutinho-Budd, J., Ghukasyan, V., Zylka, M. J. & Polleux, F. (2012). *J. Cell Sci.* **125**, 3390–3401.
Frost, A., Perera, R., Roux, A., Spasov, K., Destaing, O., Egelman, E. H., De Camilli, P. & Unger, V. M. (2008). *Cell*, **132**, 807–817.
Frost, A., Unger, V. M. & De Camilli, P. (2009). *Cell*, **137**, 191–196.
Guerrier, S., Coutinho-Budd, J., Sassa, T., Gresset, A., Jordan, N. V., Chen, K., Jin, W.-L., Frost, A. & Polleux, F. (2009). *Cell*, **138**, 990–1004.
Itoh, T., Erdmann, K. S., Roux, A., Habermann, B., Werner, H. & De Camilli, P. (2005). *Dev. Cell*, **9**, 791–804.
Lee, S. H., Kerff, F., Chereau, D., Ferron, F., Klug, A. & Dominguez, R. (2007). *Structure*, **15**, 145–155.
Ma, Y., Mi, Y.-J., Dai, Y.-K., Fu, H.-L., Cui, D.-X. & Jin, W.-L. (2013). *PLoS One*, **8**, e57865.
Matthews, B. W. (1968). *J. Mol. Biol.* **33**, 491–497.
Mattila, P. K., Pykäläinen, A., Saarikangas, J., Paavilainen, V. O., Vihinen, H., Jokitalo, E. & Lappalainen, P. (2007). *J. Cell Biol.* **176**, 953–964.
McCoy, A. J., Grosse-Kunstleve, R. W., Adams, P. D., Winn, M. D., Storoni, L. C. & Read, R. J. (2007). *J. Appl. Cryst.* **40**, 658–674.
Otwinowski, Z. & Minor, W. (1997). *Methods Enzymol.* **276**, 307–326.
Rao, Y. & Haucke, V. (2011). *Cell. Mol. Life Sci.* **68**, 3983–3993.
Shimada, A. *et al.* (2007). *Cell*, **129**, 761–772.
Tarricone, C., Xiao, B., Justin, N., Walker, P. A., Rittinger, K., Gamblin, S. J. & Smerdon, S. J. (2001). *Nature (London)*, **411**, 215–219.